N87-18859

Behavior Sensitivities for Control Augmented Structures

R.A. Manning, R.V. Lust, and L.A. Schmit
University of California at Los Angeles
Los Angeles, CA

Introduction

During the past few years it has been recognized that combining passive structural design methods with active control techniques offers the prospect of being able to find substantially improved designs (Refs. 1-3). These developments have stimulated interest in augmenting structural synthesis by adding active control system design variables to those usually considered in structural optimization. An essential step in extending the approximation concepts approach (Refs. 4-6) to control augmented structural synthesis (Ref. 7) is the development of a behavior sensitivity analysis capability for determining rates of change of dynamic response quantities with respect to changes in structural and control system design variables. Behavior sensitivity information is also useful for man-machine interactive design as well as in the context of system identification studies. In this work behavior sensitivity formulations for both steady state and transient response are presented and the quality of the resulting derivative information is evaluated.

Augmented Equations of Motion

Consider a structural/control system that can be modeled as an assemblage of frame, truss and axial actuator elements. When such a system is subjected to harmonic loading conditions the steady state response is of primary interest. It is assumed here that: (1) direct output feedback control is used; (2) actuators and sensors are collocated; and (3) the structure/control system can be represented by a linear model. Let it also be understood that the topology, geometric layout, structural material and actuator positions are preassigned parameters while section properties and gains are selected as design variables.

Dynamic analysis is carried out using the finite element method and Eq. 1 represents the equations of motion including viscous damping $[C]$, structural damping $i\gamma[K]$, harmonic applied loads $\{P(t)\}_k$ and control forces $\{N(t)\}_k$. The control forces $\{N(t)\}_k$ are given by Eq. 2, where $[G_p]_k$ and $[G_v]_k$ denote the system level position and velocity gain matrices for the k^{th} load condition. Substituting Eq. 2 into Eq. 1 gives Eq. 3, the equations of motion for the control augmented system, where $[C_A]_k$ and $[K_A]_k$, respectively (Eqs. 4 and 5) are the augmented damping and the augmented stiffness matrices for the k^{th} load condition. For the case of axial actuators used here the system level position and velocity gain matrices are easily generated following assembly procedures similar to those commonly used in finite element analysis.

$$[M]\{\ddot{X}\}_k + [C]\{\dot{X}\}_k + (1 + i\gamma)[K]\{X\}_k = \{N(t)\}_k + \{P(t)\}_k \qquad (1)$$

$$k = 1,2,...K_d$$

$$\{N(t)\}_k = -[G_v]_k\{\dot{X}\}_k - [G_p]_k\{X\}_k \qquad (2)$$

$$[M]\{\ddot{X}\}_k + [C_A]_k\{\dot{X}\}_k + [K_A]_k\{X\}_k + i\gamma[K]\{X\}_k = \{P(t)\}_k \qquad (3)$$

$$[C_A]_k = [C] + [G_v]_k \qquad (4)$$

$$[K_A]_k = [K] + [G_p]_k \qquad (5)$$

Dynamic Response Solution

The steady state dynamic response for harmonically loaded (see Eq. 6) damped structures augmented by a linear direct output feedback control system can be obtained via a frequency response analysis as follows. Substituting Eq. 6 into the control augmented equations of motion (Eq. 3) leads to Eq. 7, where the complex displacements $\{\bar{X}\}_k$ are represented by Eq. 8. It is well known that the steady state solution of Eqs. 7 has the form shown in Eq. 9. Substituting Eq. 9 into Eq. 7, eliminating $e^{i\Omega_k t}$ from both sides, and equating the real and imaginary parts leads to a partitioned matrix equation (Eq. 10). For the general case, Eq. 10 represents a 2n x 2n set of indefinite, non-symmetric linear simultaneous algebraic equations in the unknowns $\{C_R\}_k$ and $\{C_I\}_k$, where n equals the number of degrees of freedom in the system model. For the special case treated here (i.e. collocated axial actuators and sensors) the efficiency of the solution process can be improved because $[K_A]_k$ and $[C_A]_k$ are symmetric and Eq. 10 can be rewritten in the symmetric form shown in Eq. 11.

$$\{P(t)\}_k = \{P\}_k e^{i\Omega_k t} \tag{6}$$

$$[M]\{\ddot{\bar{X}}\}_k + [C_A]_k\{\dot{\bar{X}}\}_k + [K_A]_k\{\bar{X}\}_k + i\gamma[K]\{\bar{X}\}_k = \{P\}_k e^{i\Omega_k t} \tag{7}$$

$$\{\bar{X}\}_k = \{X_R\}_k + i\,\{X_I\}_k \tag{8}$$

$$\{\bar{X}\}_k = \{\bar{C}\}_k e^{i\Omega_k t} = (\{C_R\}_k + i\{C_I\}_k) e^{i\Omega_k t} \tag{9}$$

$$\left[\begin{array}{c|c} [K_A]_k - \Omega_k^2[M] & -\Omega_k[C_A]_k - \gamma[K] \\ \hline \Omega_k[C_A]_k + \gamma[K] & [K_A]_k - \Omega_k^2[M] \end{array}\right] \left\{\begin{array}{c} \{C_R\}_k \\ \hline \{C_I\}_k \end{array}\right\} = \left\{\begin{array}{c} \{P\}_k \\ \hline \{0\} \end{array}\right\} \tag{10}$$

$$k = 1,2,\ldots K_d.$$

Dynamic Response Solution (cont.)

The amplitude of the steady state dynamic displacements can be obtained as follows. Solve Eq. 11 for the primary unknowns $\{C_R\}_k$ and $\{C_I\}_k$. Note that $e^{i\Omega_k t}$ can be expressed in the alternate form given by Eq. 12. Then it follows from Eqs. 8 and 9 that the steady state dynamic response is given by Eq. 13 where $\{X_R\}_k$ and $\{X_I\}_k$ solve Eq. 1 when the loading function has the form of a cosine or a sine respectively. When the loading function is sinusoidal the amplitude of the dynamic displacement for the j^{th} degree of freedom is given by Eq. 14. It is worth noting that Eq. 14 is a relatively simple explicit nonlinear expression for the amplitude of the steady state dynamic response in terms of the primary unknowns of the analysis, namely $\{C_R\}_k$ and $\{C_I\}_k$.

$$\left[\begin{array}{c|c} \Omega_k[C_A]_k + \gamma[M] & [K_A]_k - \Omega_k^2[M] \\ \hline [K_A]_k - \Omega_k^2[M] & -\Omega_k[C_A]_k - \gamma[M] \end{array}\right] \left\{\begin{array}{c} \{C_R\}_k \\ \hline \{C_I\}_k \end{array}\right\} = \left\{\begin{array}{c} \{0\} \\ \hline \{P\}_k \end{array}\right\} \tag{11}$$

$$e^{i\Omega kt} = \cos\Omega_k t + i \sin \Omega_k t \tag{12}$$

$$\{\bar{X}\}_k = \{X_R\}_k + i\{X_I\}_k = (\{C_R\}_k \cos\Omega_k t - \{C_I\}_k \sin\Omega_k t)$$

$$+ i(\{C_R\}_k \sin\Omega_k t + \{C_I\}_k \cos\Omega_k t) \tag{13}$$

$$\left| X_{Ijk} \right| = \left[C_{Rjk}^2 + C_{Ijk}^2\right]^{1/2} \tag{14}$$

Behavior Sensitivity Analysis

Approximate values of the amplitude for the j^{th} degree of freedom under the k^{th} load condition ($|\tilde{X}_{jk}|$) will be obtained by constructing first order Taylor series approximations for the primary unknowns of the steady state response, namely $\tilde{C}_{Rjk}$ and $\tilde{C}_{Ijk}$. Equations (15a) and (15b) show the first order Taylor series approximations for the primary unknowns of the steady state response analysis and they are linear in the design variables (i.e. element properties). Note that the subscript 0 refers to the base design for which an analysis is available. Substituting Eqs. (15 a,b) into Eq. (14')gives the desired explicit approximation for the amplitude of the j^{th} degree of freedom under the k^{th} load condition. It is apparent that the first partial derivatives of the primary unknowns evaluated at the base design must be known in order to evaluate approximate values of the amplitude. These behavior sensitivity derivatives are readily found by implicit differentiation of Eq. 11' (i.e. Eq. 11 written in compact notation where $[A]_k = \Omega_k[C_A]_k + \gamma[M]$ and $[B]_k = [K_A]_k - \Omega_k^2\,[M]$) with respect to the design variables d_r, which leads to Eq. 16.

$$|\tilde{X}_{jk}| = (\tilde{C}^2_{Rjk} + \tilde{C}^2_{Ijk})^{1/2} \tag{14'}$$

$$\tilde{C}_{Rjk} = (C_{Rjk})_o + \sum_r \left[\frac{\partial C_{Rjk}}{\partial d_r}\right]_o \left[d_r - d_{ro}\right] \tag{15a}$$

$$\tilde{C}_{Ijk} = (C_{Ijk})_o + \sum_r \left[\frac{\partial C_{Ijk}}{\partial d_r}\right]_o \left[d_r - d_{ro}\right] \tag{15b}$$

$$\begin{bmatrix} [A] & [B] \\ [B] & -[A] \end{bmatrix}_k \begin{Bmatrix} \{C_R\}_k \\ \{C_I\}_k \end{Bmatrix} = \begin{Bmatrix} \{0\} \\ \{P\}_k \end{Bmatrix} \tag{11'}$$

$$\begin{bmatrix} \frac{\partial[A]}{\partial d_r} & \frac{\partial[B]}{\partial d_r} \\ \frac{\partial[B]}{\partial d_r} & \frac{\partial[A]}{\partial d_r} \end{bmatrix}_k \begin{Bmatrix} \{C_R\}_k \\ \{C_I\}_k \end{Bmatrix} + \begin{bmatrix} [A] & [B] \\ [B] & -[A] \end{bmatrix}_k \begin{Bmatrix} \frac{\partial\{C_R\}_k}{\partial d_r} \\ \frac{\partial\{C_I\}_k}{\partial d_r} \end{Bmatrix} = \begin{Bmatrix} \{0\} \\ \{0\} \end{Bmatrix} \tag{16}$$

Behavior Sensitivity Analysis (cont.)

Equation 16 is written in a more compact notation in Eq. 17 and it becomes apparent on examining Eq. 17 that the form of this sensitivity analysis is very similar to that which arises for the case of linear static analysis (i.e. $K \frac{\partial\{X\}_k}{\partial d_r} = \{V\}_{rk} = -\left[\frac{\partial K}{\partial d_r}\right]\{X\}_k$). The terms on the right hand side of Eq. 17 play the role of pseudo-load vectors that are easily evaluated once the primary unknowns of the analysis have been determined for a base design by solving Eq. 11. The solution of Eq. 17 for the desired first derivatives $\left[\frac{\partial\{C_R\}_k}{\partial d_r} \text{ and } \frac{\partial\{C_I\}_k}{\partial d_r}\right]$ require relatively little effort because the 2n x 2n matrix in Eq. 17 was previously decomposed into LDL^T form when the primary analysis was executed by solving Eq. 11. Furthermore, the computational efficiency of the primary sensitivity analysis (solving Eq. 17) can be enhanced by employing the well known partial inverse method to obtain only the desired partial derivatives. (Ref. 5).

$$\left[\begin{array}{c|c} [A] & [B] \\ \hline [B] & -[A] \end{array}\right]_k \left\{\begin{array}{c} \dfrac{\partial\{C_R\}_k}{\partial d_r} \\ \hline \dfrac{\partial\{C_I\}_k}{\partial d_r} \end{array}\right\} = \left\{\begin{array}{c} \{V_I\}_{rk} \\ \hline \{V_R\}_{rk} \end{array}\right\} \tag{17}$$

$$\{V_I\}_{rk} = -\frac{\partial[A]_k}{\partial d_r}\{C_R\}_k - \frac{\partial[B]_k}{\partial d_r}\{C_I\}_k \tag{18}$$

$$\{V_R\}_{rk} = -\frac{\partial[B]_k}{\partial d_r}\{C_R\}_k + \frac{\partial[A]_k}{\partial d_r}\{C_I\}_k \tag{19}$$

$$\frac{\partial}{\partial d_r}[A]_k = \frac{\partial}{\partial d_r}\left[\Omega_k[C_A]_k + \gamma[K]\right] = \Omega_k \frac{\partial[C_A]_k}{d_r} + \gamma \frac{\partial[K]}{\partial d_r} \tag{20}$$

$$\frac{\partial}{\partial d_r}[B]_k = \frac{\partial}{\partial d_r}\left[[K_A]_k - \Omega_k^2 M\right] = \frac{\partial[K_A]_k}{\partial d_r} - \Omega_k^2 \frac{\partial[M]}{\partial d_r} \tag{21}$$

Numerical Example - Steady-State Response

The quality of the steady state dynamic response behavior sensitivities is evaluated for the planar grillage shown in Figure 1. The grillage consists of nine aluminum box beams and is cantilevered at node 1. A dynamic load P(t) = 100.0 N sin (5.0 Hz)t is applied slightly off the centerline of the grillage at node 8 so that both symmetric and anti-symmetric modes participate in the response. Three active control elements placed at nodes 5, 6, and 7 act in the vertical direction. Two percent structural damping is assumed.

Taylor series approximations based on direct and reciprocal element properties are compared with the exact results for the maximum steady state vertical displacements at node 7 for various design variables (See Figures 2 through 6). One can see that the difference between the approximations and the exact displacements is relatively small even when considering 30 to 40% changes in the primary load-carrying member (i.e., 30 to 40% changes in the bending inertia for element 1).

In order to study the behavior of the approximations in a near-resonance condition, a harmonic loading of frequency 20 Hz is applied at node 8. This loading will excite the flapping - type 5th mode (f_5 = 19.63 Hz) of the grillage.

Figures 7 and 8 bring out two major difficulties associated with resonance or near-resonance situations: (1) the high nonlinearity of the exact response curve; and (2) the nonconvexity of the design space. Nonlinearity of the response curve results in the Taylor series approximations being of acceptable quality in only a limited interval near the base point (i.e. ± 10%). Nonconvexity of the design space could lead to local minima in an optimization context. These difficulties lead one to use frequency constraints to avoid the near-resonance conditions in optimum design problems.

Transient Response Equations of Motion

In applications where the external loading is either not harmonic or cannot be conservatively replaced with an equivalent harmonic loading, peak transient response is a primary concern. Furthermore, nonlinear on/off controls are well suited to controlling transient response and they are practical for space-based structures.

The dynamic equations of motion for a finite element representation of a linear structure augmented by a discrete actuator control system are given in equation 22 where $\{P(t)\}$ is the nodal load time history, $\{u\}$ is a vector of actuator output forces, and [B] is a matrix of zeroes and ones locating the discrete actuators at nodal degrees of freedom. Vectors of observed displacements and velocities, $\{Y\}$ and $\{\dot{Y}\}$, respectively, are available from the control system sensors and are given in equation 23 where [C] is a matrix of zeroes and ones locating the discrete sensors at nodal degrees of freedom. The actuator output forces, $\{u\}$, are chosen in a manner which reduces the system response based on the sensor measurements. In particular, the output force for the nth actuator is given in equation 24 where $\bar{u}_n$ is the output magnitude for the control system and ε_n is the velocity threshold.

Transformation of equation 22 from physical space to modal space yields equation 25b where modal damping has been introduced into the system through the ζ parameter. The uncoupled modal equations in 25b are easily solved for the modal coordinates using the Wilson-θ time-stepping scheme and physical displacements are recovered using the modal transformation in 25a.

The kth modal second order equation of motion can be written in the equivalent first order form given by equation 26 where $n_1 = q$ and $n_2 = \dot{q}$.

$$[M]\{\ddot{X}\} + [K]\{X\} = \{P(t)\} + [B]\{u\} \tag{22}$$

$$\{Y\} = [C]\{X\} \qquad \{\dot{Y}\} = [C]\{\dot{X}\} \tag{23}$$

$$u_n = \begin{cases} 0 & \text{if } |\dot{Y}_n| \le \varepsilon_n \\ -\bar{u}_n & \text{if } |\dot{Y}_n| \ge \varepsilon_n \text{ and } \dot{Y}_n > 0 \\ \bar{u}_n & \text{if } |\dot{Y}_n| \ge \varepsilon_n \text{ and } \dot{Y}_n < 0 \end{cases} \tag{24}$$

$$\{X\} = [\phi]\{q\} \quad (25a) \qquad \ddot{q}_k + 2\zeta_k\omega_k\dot{q} + \omega_k^2 q = Q_k + Z_k \tag{25b}$$

$$\begin{Bmatrix} \dot{n}_1 \\ \dot{n}_2 \end{Bmatrix}_k = \begin{bmatrix} 0 & 1 \\ -\omega_k^2 & -2\zeta_k\omega_k \end{bmatrix} \begin{Bmatrix} n_1 \\ n_2 \end{Bmatrix}_k + \begin{Bmatrix} 0 \\ 1 \end{Bmatrix} Q_k + \begin{Bmatrix} 0 \\ 1 \end{Bmatrix} Z_k \tag{26}$$

Calculation of Behavior Sensitivities

Time dependent transient response sensitivities can be obtained by differentiating the modal transformation given in equation 25a with respect to each design variable (beam element section properties and actuator output force levels) to yield equation 27. The first term in equation 27 is known from the system response solution and the eigenvector sensitivities. The $\{\frac{\partial q}{\partial d_r}\}$ quantity in the second term is the last desired quantity.

The direct way of obtaining these partial derivatives is to differentiate equation 26 (or equation 25b) with respect to each design variable to obtain equation 28 and time step on these equations. The computational effort needed to obtain $\{\frac{\partial q}{\partial d_r}\}$ would be KR time stepping solutions where K is the number of retained modes and R is the number of independent design variables.

A more efficient way to obtain this last desired quantity is to exploit the special form of equation 26 by applying the Wilkie-Perkins essential parameter method (Ref. 8). Writing equation 26 in compact notation yields equation 29a where the [A] matrix in equation 29b is in Frobenius canonical form with $\alpha_1 = \omega^2$ and $\alpha_2 = 2\zeta\omega$ being referred to as essential parameters. A sensitivity matrix $[\xi]$ can be defined as in equation 30. As a consequence of the [A] matrix being in canonical form, two beneficial properties of the sensitivity matrix are: (1) the sensitivity matrix has a total symmetry property resulting in all terms on a single anti-diagonal being equal; and (2) the sensitivity matrix has a complete simultaneity property resulting in all sensitivity functions for the canonical system being linear combinations of the modal response, n_1 and n_2, and $\frac{\partial n_1}{\partial \alpha_1}$ and $\frac{\partial n_1}{\partial \alpha_2}$. The equations shown in 31a and 31b result from these two properties.

$$\left\{\frac{\partial X}{\partial d_r}\right\} = \left[\frac{\partial \phi}{\partial d_r}\right]\{q\} + [\phi]\left\{\frac{\partial q}{\partial d_r}\right\} \tag{27}$$

$$\begin{Bmatrix} \frac{\partial \dot{n}_1}{\partial d_r} \\ \frac{\partial \dot{n}_2}{\partial d_r} \end{Bmatrix}_k = \begin{bmatrix} 0 & 0 \\ -\frac{\partial \omega_k^2}{\partial d_r} & -\frac{\partial (2\zeta_k \omega_k)}{\partial d_r} \end{bmatrix} \begin{Bmatrix} n_1 \\ n_2 \end{Bmatrix}_k + \begin{bmatrix} 0 & 1 \\ -\omega_k^2 & -2\zeta\omega_k \end{bmatrix} \begin{Bmatrix} \frac{\partial n_1}{\partial d_r} \\ \frac{\partial n_2}{\partial d_r} \end{Bmatrix}_k + \begin{Bmatrix} 0 \\ 1 \end{Bmatrix} \frac{\partial Q_k}{\partial d_r} + \begin{Bmatrix} 0 \\ 1 \end{Bmatrix} \frac{\partial Z_k}{\partial d_r} \tag{28}$$

$$\{\dot{n}\} = [A]\{n\} + \{b\}\,Q + \{b\}\,Z \quad (29a) \qquad A = \begin{bmatrix} 0 & 1 \\ -\alpha_1 & -\alpha_2 \end{bmatrix} \tag{29b}$$

$$[\xi] = \begin{bmatrix} \frac{\partial n_1}{\partial \alpha_1} & \frac{\partial n_1}{\partial \alpha_2} \\ \frac{\partial n_2}{\partial \alpha_1} & \frac{\partial n_2}{\partial \alpha_2} \end{bmatrix} \tag{30}$$

$$\frac{\partial n_1}{\partial \alpha_2} = \frac{\partial n_2}{\partial \alpha_1} \quad (31a) \qquad \frac{\partial n_2}{\partial \alpha_2} = -n_1 - \alpha_1 \frac{\partial n_1}{\partial \alpha_1} - \alpha_2 \frac{\partial n_2}{\partial \alpha_1} - \alpha_2 \frac{\partial n_1}{\partial \alpha_2} \tag{31b}$$

Calculation of Behavior Sensitivities (cont.)

Evaluation of the $\{\frac{\partial q}{\partial d_r}\}$ term utilizing the Wilkie-Perkins essential parameter method is done by: (1) differentiating equation 29a with respect to α_1 to yield equation 32; (2) time stepping on equation 32; (3) chain ruling from essential parameter space to design variable space via equation 33. Thus the computational effort needed to obtain $\{\frac{\partial q}{\partial d_r}\}$ has been reduced from KR time stepping solutions to K.

It should be noted that this method of obtaining behavior sensitivities can only be used for the passive structural design variables since the essential parameters are independent of the active control design variables. Sensitivities of the transient dynamic response with respect to the active control design variables can be obtained by differentiating equation 26 with respect to the active control design variables to yield 34. Equation 34 is time-stepped for the desired terms.

$$\begin{Bmatrix} \frac{\partial \dot{n}_1}{\partial \alpha_1} \\ \frac{\partial \dot{n}_2}{\partial \alpha_1} \end{Bmatrix} = \begin{bmatrix} 0 & 0 \\ -1 & 0 \end{bmatrix} \begin{Bmatrix} n_1 \\ n_2 \end{Bmatrix} + \begin{bmatrix} 0 & 1 \\ -\alpha_1 & -\alpha_2 \end{bmatrix} \begin{Bmatrix} \frac{\partial n_1}{\partial \alpha_1} \\ \frac{\partial n_2}{\partial \alpha_1} \end{Bmatrix} \tag{32}$$

$$\left\{ \frac{\partial q}{\partial d_r} \right\} = \frac{\partial q}{\partial \alpha_1} \frac{\partial \alpha_1}{\partial d_r} + \frac{\partial q}{\partial \alpha_2} \frac{\partial \alpha_2}{\partial d_r} \tag{33}$$

$$\begin{Bmatrix} \frac{\partial \dot{n}_1}{\partial d_r} \\ \frac{\partial \dot{n}_2}{\partial d_r} \end{Bmatrix}_k = \begin{bmatrix} 0 & 1 \\ -\omega_k^2 & -2\zeta_k\omega_k \end{bmatrix} \begin{Bmatrix} \frac{\partial n_1}{\partial d_r} \\ \frac{\partial n_2}{\partial d_r} \end{Bmatrix}_k + \left\{ b \right\} \frac{\partial Z_k}{\partial d_r} \tag{34}$$

Numerical Example - Transient Response

The same aluminum planar grillage (see Fig. 1) used for the steady state response sensitivities is used to examine the quality of the peak transient response sensitivities. The loading consists of the force time history shown in Figure 9 applied at node 8. A single collocated sensor/actuator pair is located at node 6 and acts in the vertical direction. Peak transient response and peak transient response sensitivities were calculated by time-stepping through 1 second in 0.0005 second increments using ten retained modes (frequency content up to 100 Hz) and 2% modal damping.

Exact results for the peak positive and negative displacements at nodes 5 and 7 are compared with both direct and reciprocal element property Taylor series approximations in Figures 10 through 22 for a number of different design variables. For design variable changes up to ±20% the approximations are seen to be of acceptable accuracy. Furthermore, the direct approximations for peak displacements as functions of the actuator force level agree extremely well with the exact response curve (see Figures 19 through 22).

It should be noted that the degree of conservatism present in either the direct or the reciprocal section property approximations is not necessarily correlated with its accuracy. For instance, in Figure 15, the reciprocal approximation is more conservative than the direct approximation, but is far less accurate for design variable changes greater than 20%.

Conclusions

In this work behavior sensitivity formulations for both steady state and transient response were developed and the quality of the resulting derivative information was assessed.

Derivatives of the steady state response with respect to both structural and control design variables for harmonically loaded structures augmented by a linear direct output feedback control system were presented. The base design dynamic response was calculated using a frequency response method which reduced the solution of the complex dynamical equations of motion to the solution of a 2n x 2n set of linear algebraic equations. The response quantity sensitivities were obtained directly using the psuedo-load method in its partial inverse form. Taylor series approximations in both direct and reciprocal element properties were constructed using this sensitivity information and shown to yield high quality approximations for 30 to 40% design variable changes provided near-resonance conditions are not encountered. When resonance or near-resonance conditions are present, the approximations for the response quantities are of acceptable quality for a relatively restricted interval around the base design.

Using a normal mode method of analysis, peak transient response and peak transient response sensitivities were calculated for arbitrarily loaded structures augmented by nonlinear on/off control actuators. The special form of the modal equations of motion was exploited to reduce the computational effort needed to obtain transient response sensitivities. These sensitivities were used to construct Taylor series approximations in both direct and reciprocal element properties for peak transient response. The approximations are of acceptable quality for structural design variable changes of up to 20%. The direct approximations in terms of the controller variables compare very well with the exact response for up to 50% changes in the design variables.

The results of this paper show that for control augmented structural systems, high quality approximations for both steady state dynamic response and peak transient response can be constructed. Therefore, the approximation concepts approach for structural synthesis can be extended to include both steady state dynamic response (Ref. 7) and peak transient response.

References

1. Venkayya, V.B. and Tischler, V.A., "Frequency Control and the Effect on Dynamic Response of Flexible Structures," *Proceedings of the 25th AIAA/ASME/ASCE/AHS Structures, Structural Dynamics and Materials Conference*, Palm Springs, California, May 14-16, 1984, pp. 431-441.

2. Haftka, R.T., Martinovic, Z.N. and Hallauer, W.L., "Enhanced Vibration Controllability by Minor Structural Modifications," AIAA Journal, Vol. 23, No. 8, August, 1985, pp. 1260-1266.

3. Haftka, R.T., Martinovic, Z.N., Hallauer, W.L. and Schamel, G., "Sensitivity of Optimized Control Systems to Minor Structural Modification," *Proceedings of the 26th AIAA/ASME/ASCE/AHS Structures, Structural Dynamics and Materials Conference,* Orlando, Florida, April 15-17, 1985, pp. 642-650.

4. Schmit, L.A. and Farshi, B., "Some Approximation Concepts for Efficient Structural Synthesis," *AIAA Journal,* Vol. 12, No. 5, 1974, pp. 692-699.

5. Schmit, L.A. and Miura, H., "Approximation Concepts for Efficient Structural Synthesis," NASA CR 2552, March, 1976.

6. Lust, R.V. and Schmit, L.A., "Alternative Approximation Concepts for Space Frame Synthesis," *Proceedings of the 26th AIAA/ASME/ASCE/AHS Structures, Structural Dynamics and Materials Conference,* Orlando, Florida, April 15-17, 1985, pp. 333-348.

7. Lust, R.V. and Schmit, L.A., "Control Augmented Structural Synthesis", AIAA Paper No. 86-1014-CP, presented at the 27th AIAA/ASME/ASCE/AHS Structures, Structural Dynamics, and Materials Conference, San Antonio, Texas, May 19-21, 1986.

8. Wilkie, D.F. and Perkins, W.R., "Essential Parameters in Sensitivity Analysis", *Automatica,* Vol. 5, 1969, pp. 191-197.

PLANAR GRILLAGE STRUCTURE

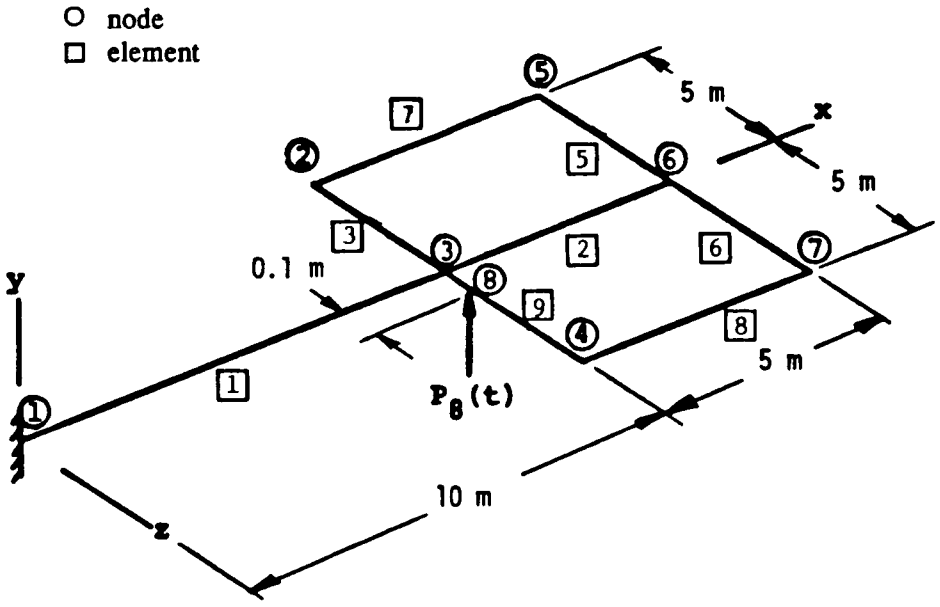

Fig. 1

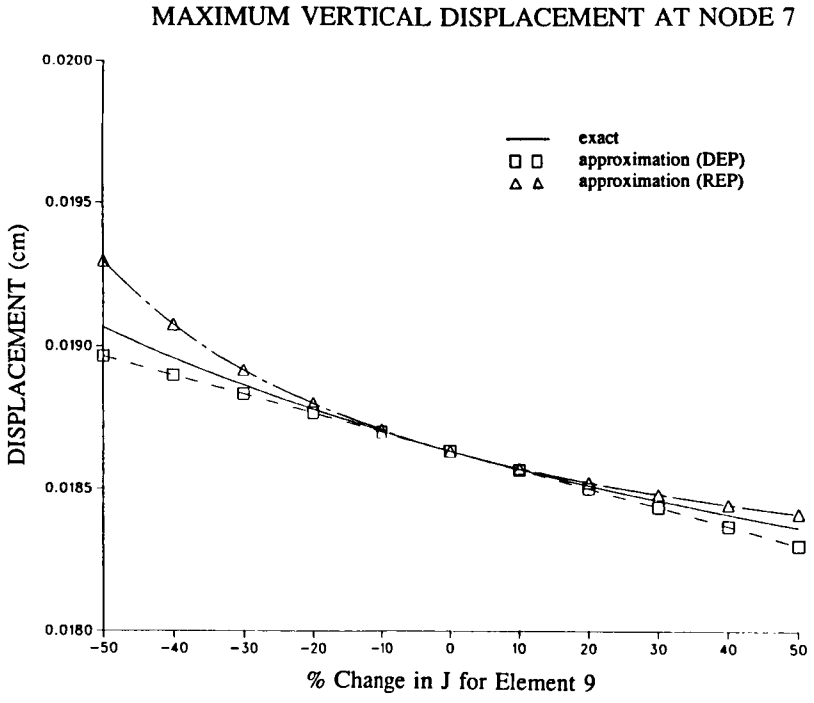

Fig. 2

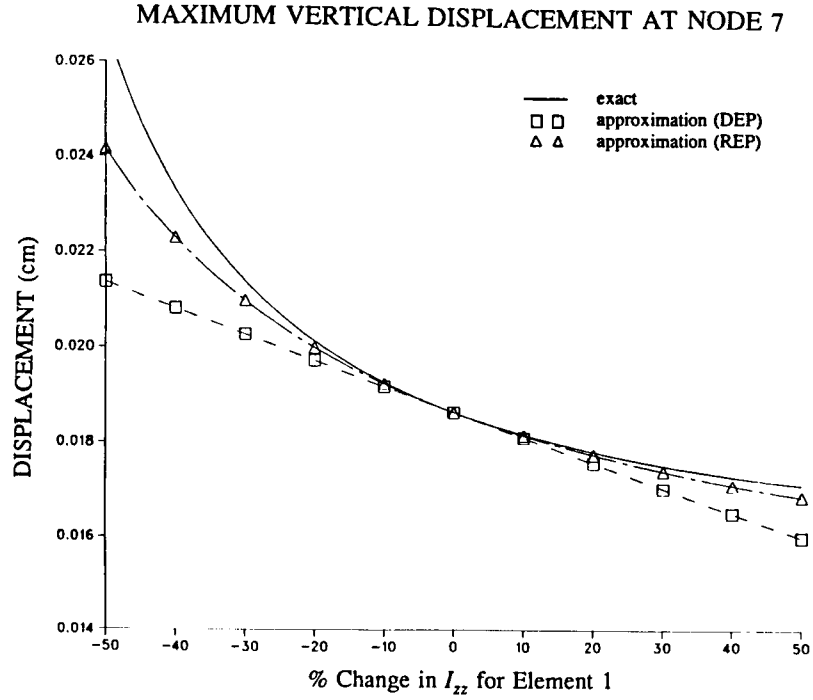
MAXIMUM VERTICAL DISPLACEMENT AT NODE 7
exact
approximation (DEP)
approximation (REP)
DISPLACEMENT (cm)
0.026
0.024
0.022
0.020
0.018
0.016
0.014
-50
-40
-30
-20
-10
0
10
20
30
40
50
% Change in I_{zz} for Element 1

Fig. 3

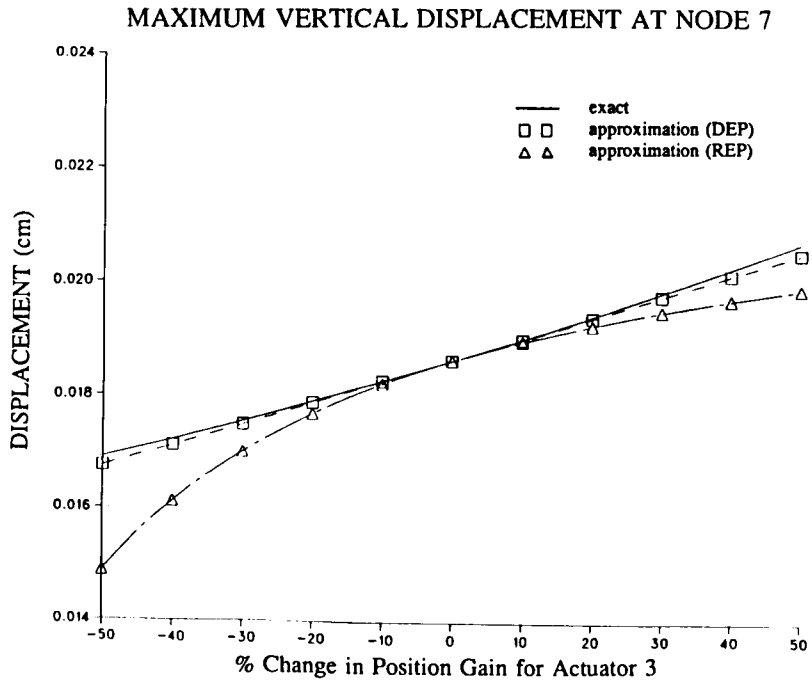
MAXIMUM VERTICAL DISPLACEMENT AT NODE 7
exact
approximation (DEP)
approximation (REP)
DISPLACEMENT (cm)
0.024
0.022
0.020
0.018
0.016
0.014
-50
-40
-30
-20
-10
0
10
20
30
40
50
% Change in Position Gain for Actuator 3

Fig. 4

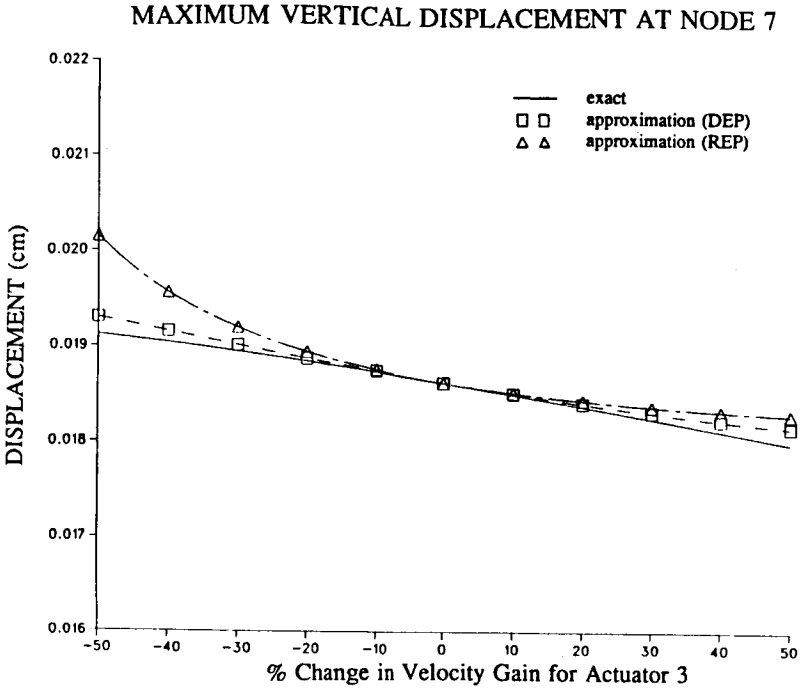
MAXIMUM VERTICAL DISPLACEMENT AT NODE 7
exact
approximation (DEP)
approximation (REP)
DISPLACEMENT (cm)
0.022
0.021
0.020
0.019
0.018
0.017
0.016
-50
-40
-30
-20
-10
0
10
20
30
40
50
% Change in Velocity Gain for Actuator 3

Fig. 5

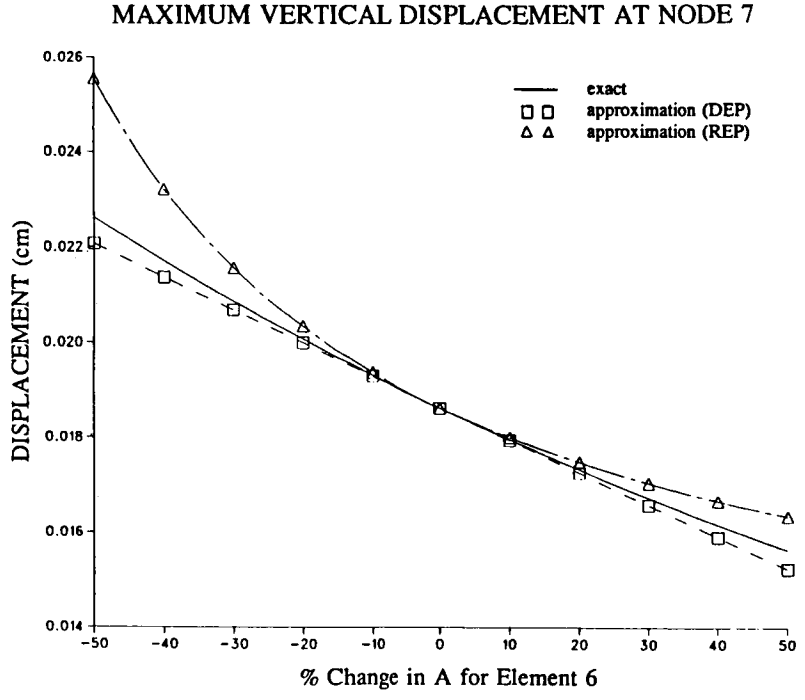
MAXIMUM VERTICAL DISPLACEMENT AT NODE 7
exact
approximation (DEP)
approximation (REP)
DISPLACEMENT (cm)
0.026
0.024
0.022
0.020
0.018
0.016
0.014
-50
-40
-30
-20
-10
0
10
20
30
40
50
% Change in A for Element 6

Fig. 6

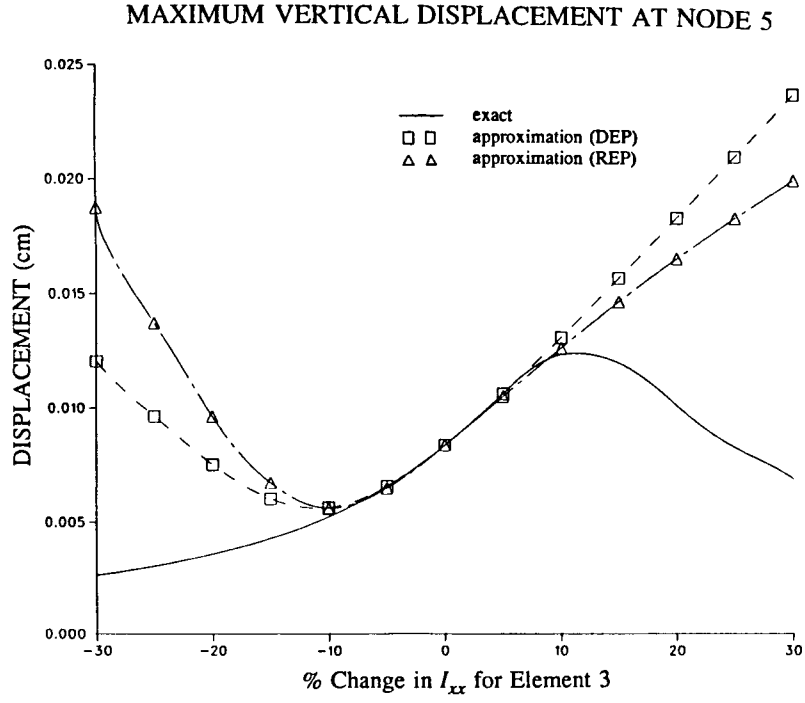
MAXIMUM VERTICAL DISPLACEMENT AT NODE 5
exact
approximation (DEP)
approximation (REP)
DISPLACEMENT (cm)
0.025
0.020
0.015
0.010
0.005
0.000
-30
-20
-10
0
10
20
30
% Change in I_{xx} for Element 3

Fig. 7

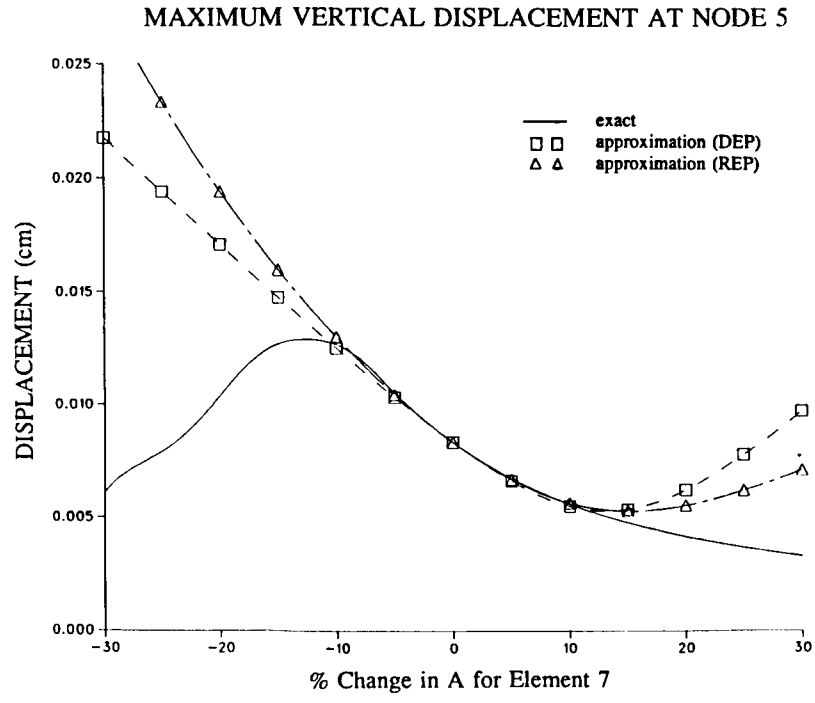
MAXIMUM VERTICAL DISPLACEMENT AT NODE 5
exact
approximation (DEP)
approximation (REP)
DISPLACEMENT (cm)
0.025
0.020
0.015
0.010
0.005
0.000
-30
-20
-10
0
10
20
30
% Change in A for Element 7

Fig. 8

APPLIED LOAD TIME HISTORY

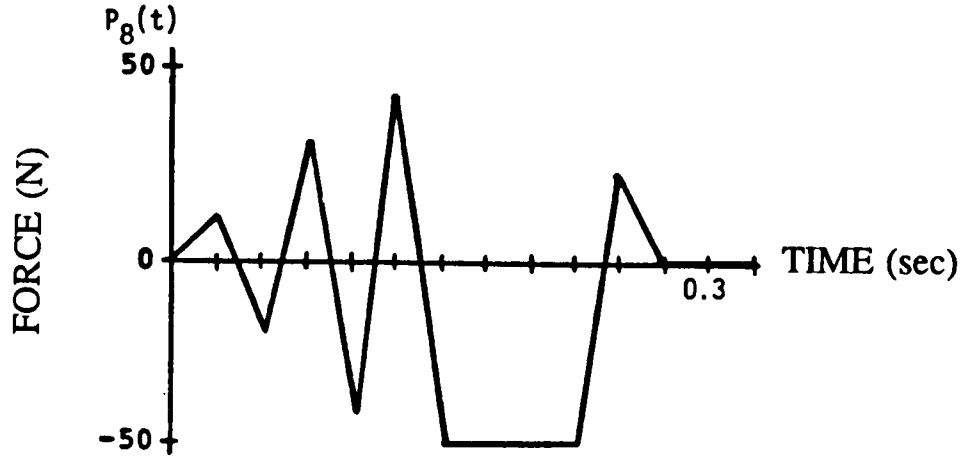

Fig. 9

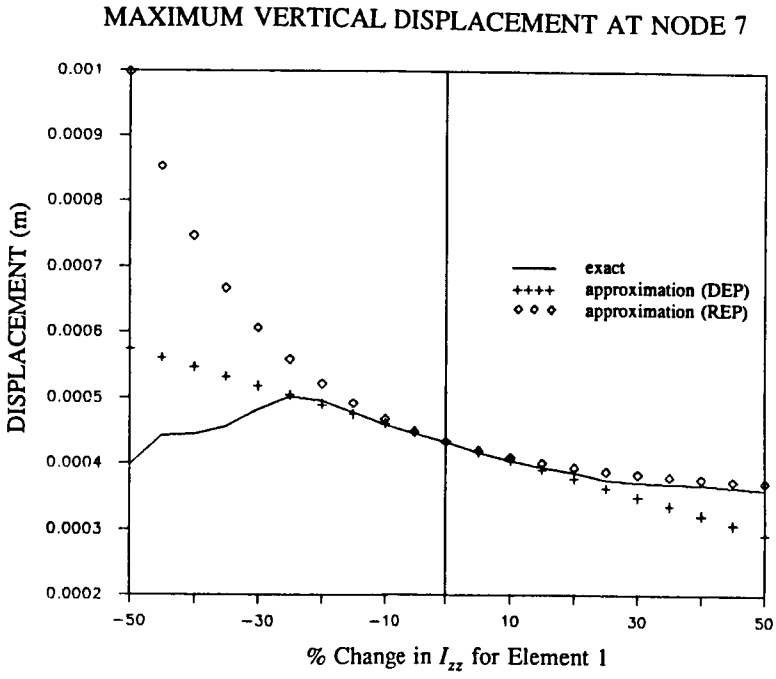

Fig. 10

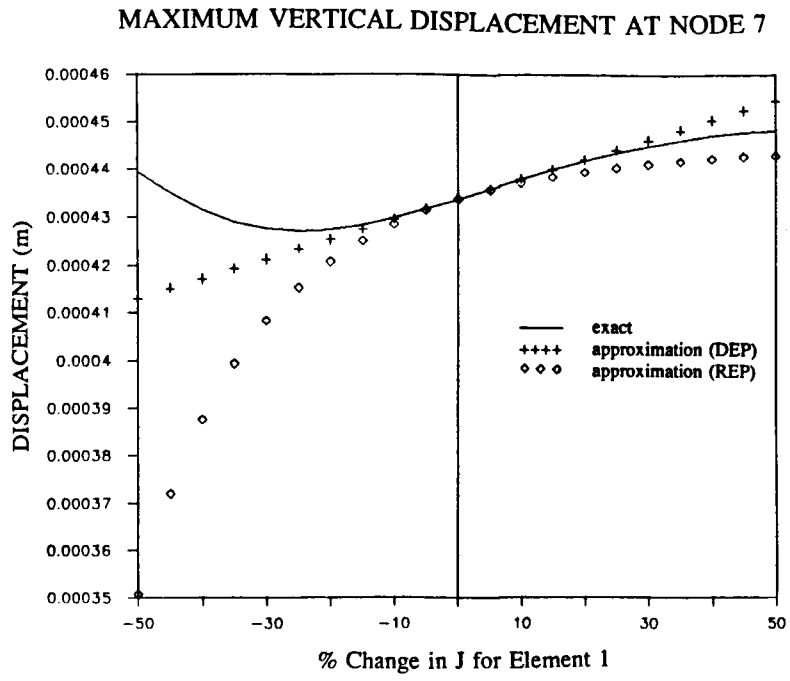
MAXIMUM VERTICAL DISPLACEMENT AT NODE 7
DISPLACEMENT (m)
0.00046
0.00045
0.00044
0.00043
0.00042
0.00041
0.0004
0.00039
0.00038
0.00037
0.00036
0.00035
-50
-30
-10
10
30
50
% Change in J for Element 1
exact
approximation (DEP)
approximation (REP)

Fig. 11

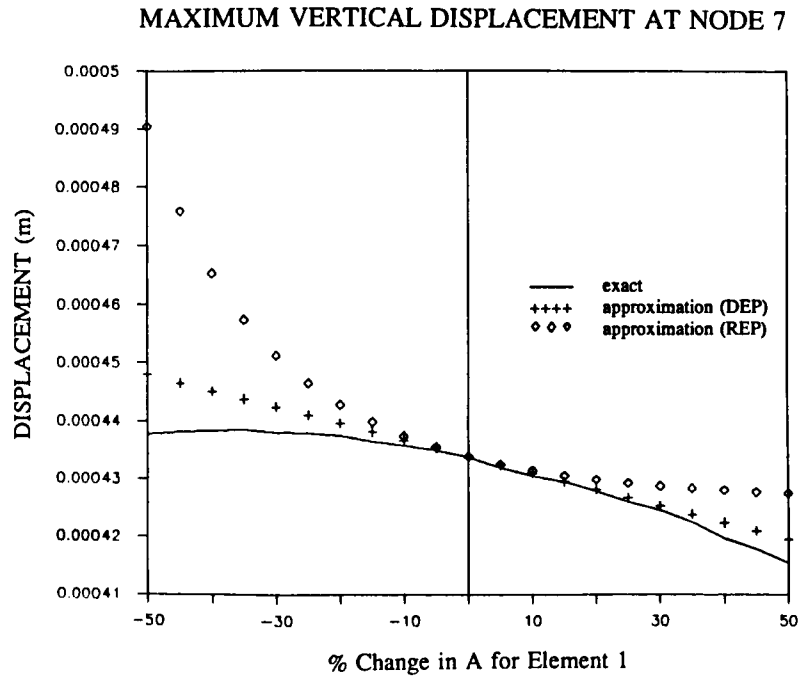
MAXIMUM VERTICAL DISPLACEMENT AT NODE 7
DISPLACEMENT (m)
0.0005
0.00049
0.00048
0.00047
0.00046
0.00045
0.00044
0.00043
0.00042
0.00041
-50
-30
-10
10
30
50
% Change in A for Element 1
exact
approximation (DEP)
approximation (REP)

Fig. 12

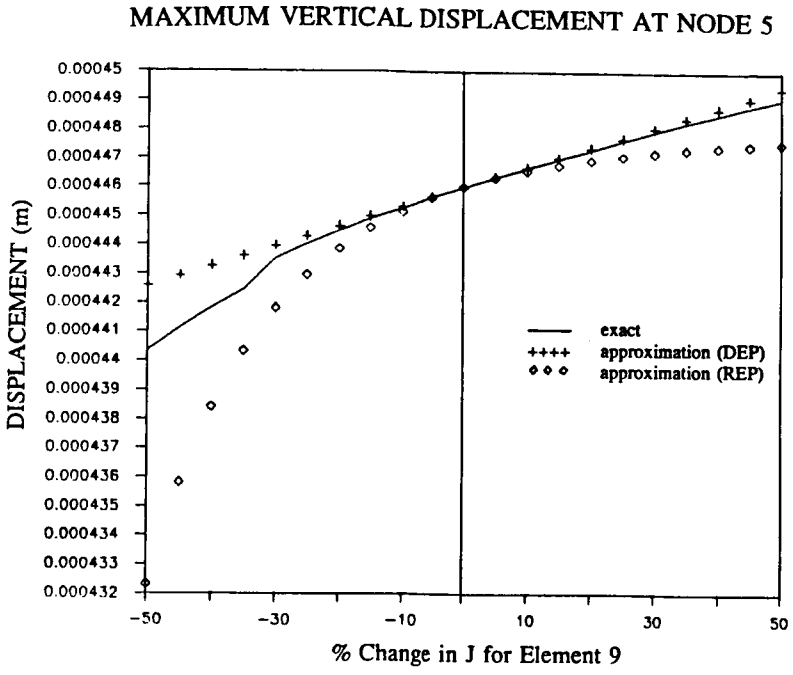
MAXIMUM VERTICAL DISPLACEMENT AT NODE 5
DISPLACEMENT (m)
0.00045
0.000449
0.000448
0.000447
0.000446
0.000445
0.000444
0.000443
0.000442
0.000441
0.00044
0.000439
0.000438
0.000437
0.000436
0.000435
0.000434
0.000433
0.000432
-50
-30
-10
10
30
50
% Change in J for Element 9
exact
approximation (DEP)
approximation (REP)

Fig. 13

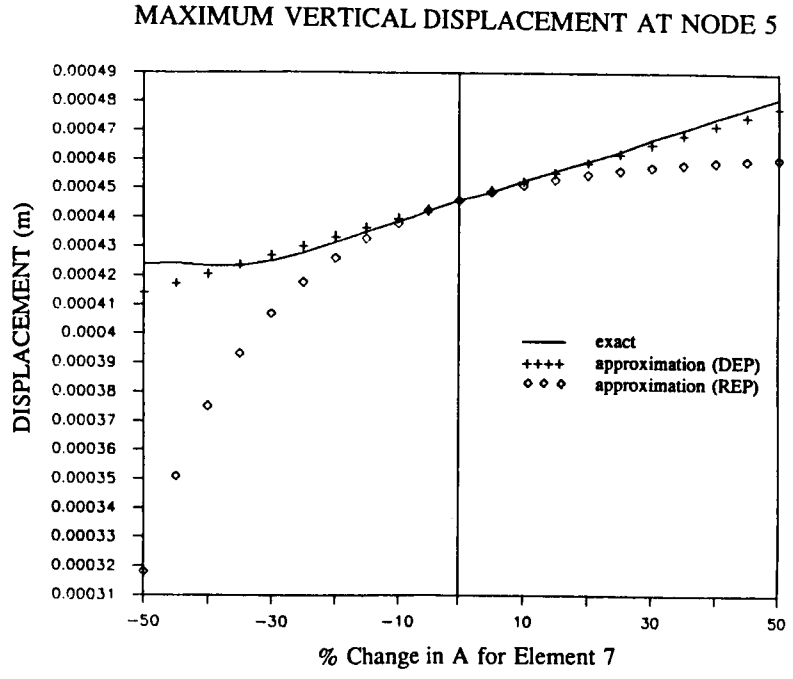
MAXIMUM VERTICAL DISPLACEMENT AT NODE 5
DISPLACEMENT (m)
0.00049
0.00048
0.00047
0.00046
0.00045
0.00044
0.00043
0.00042
0.00041
0.0004
0.00039
0.00038
0.00037
0.00036
0.00035
0.00034
0.00033
0.00032
0.00031
-50
-30
-10
10
30
50
% Change in A for Element 7
exact
approximation (DEP)
approximation (REP)

Fig. 14

MAXIMUM VERTICAL DISPLACEMENT AT NODE 5

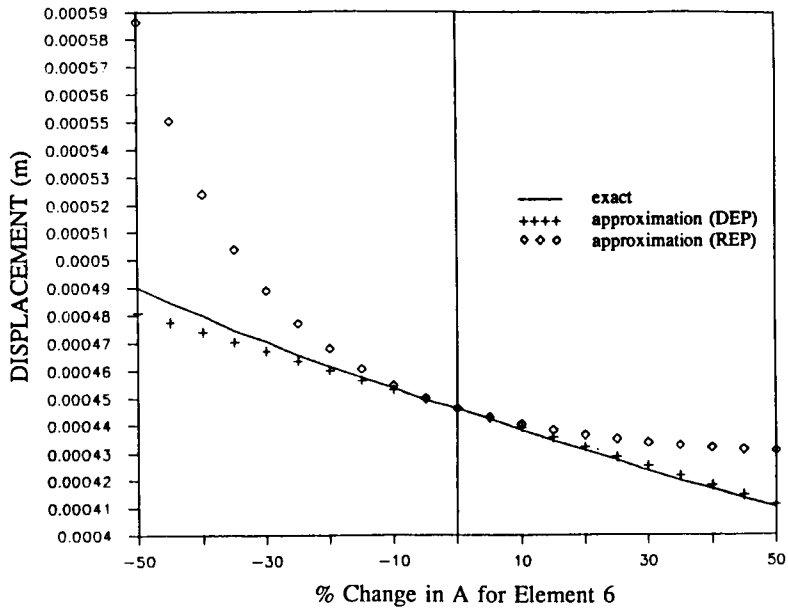

Fig. 15

MINIMUM VERTICAL DISPLACEMENT AT NODE 7

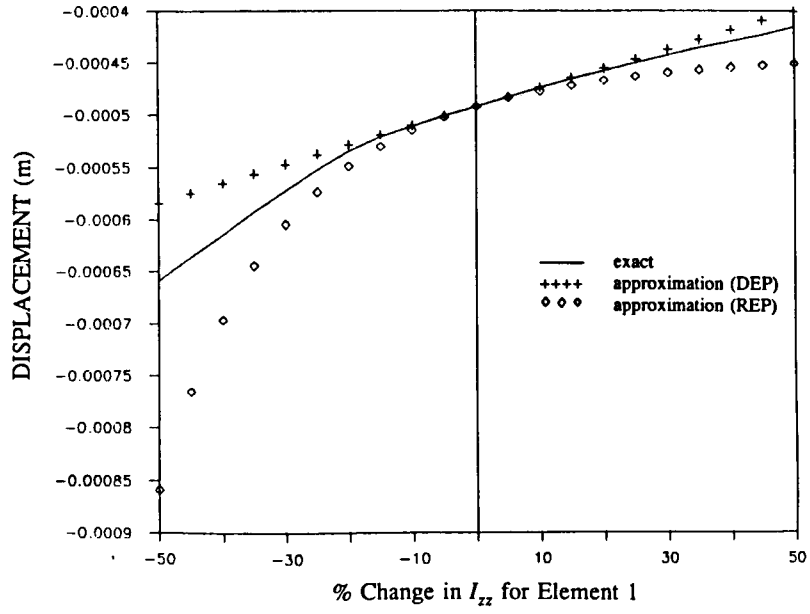

Fig. 16

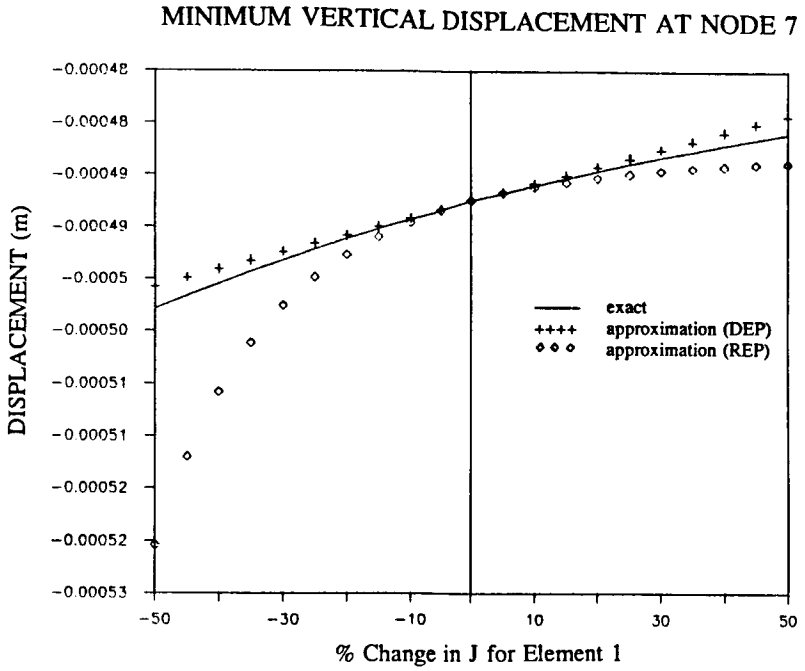
MINIMUM VERTICAL DISPLACEMENT AT NODE 7
DISPLACEMENT (m)
-0.00048
-0.00048
-0.00049
-0.00049
-0.0005
-0.00050
-0.00051
-0.00051
-0.00052
-0.00052
-0.00053
-50
-30
-10
10
30
50
% Change in J for Element 1
exact
approximation (DEP)
approximation (REP)

Fig. 17

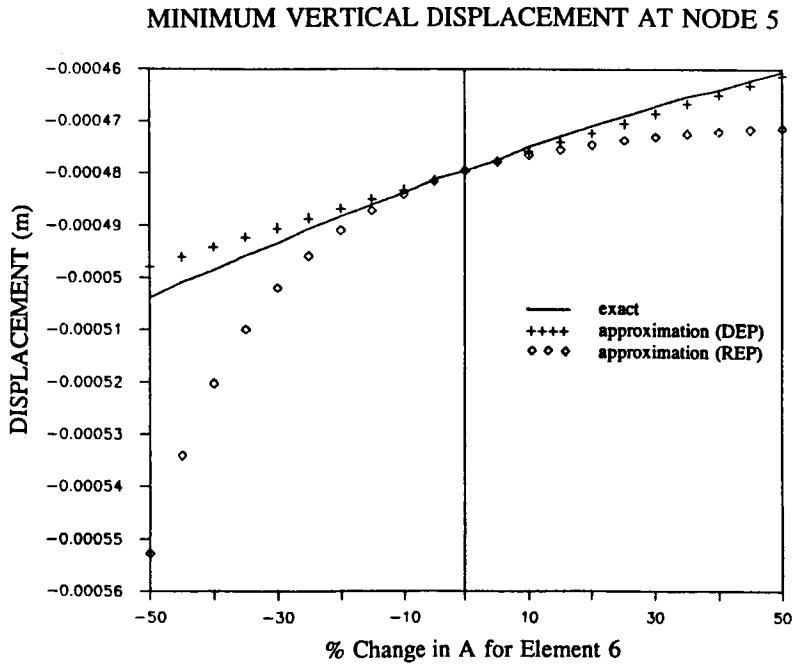
MINIMUM VERTICAL DISPLACEMENT AT NODE 5
DISPLACEMENT (m)
-0.00046
-0.00047
-0.00048
-0.00049
-0.0005
-0.00051
-0.00052
-0.00053
-0.00054
-0.00055
-0.00056
-50
-30
-10
10
30
50
% Change in A for Element 6
exact
approximation (DEP)
approximation (REP)

Fig. 18

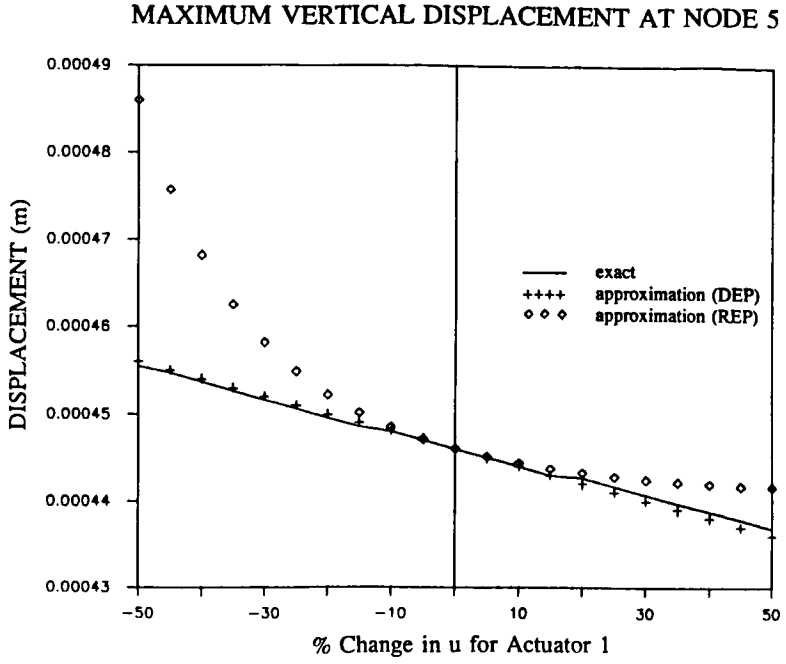
MAXIMUM VERTICAL DISPLACEMENT AT NODE 5
DISPLACEMENT (m)
0.00049
0.00048
0.00047
0.00046
0.00045
0.00044
0.00043
exact
approximation (DEP)
approximation (REP)
-50
-30
-10
10
30
50
% Change in u for Actuator 1

Fig. 19

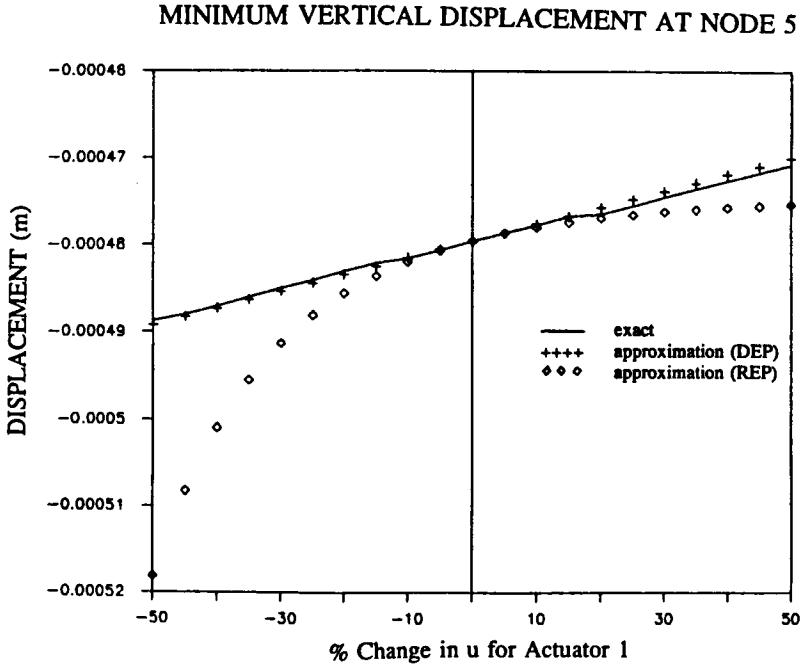
MINIMUM VERTICAL DISPLACEMENT AT NODE 5
DISPLACEMENT (m)
-0.00046
-0.00047
-0.00048
-0.00049
-0.0005
-0.00051
-0.00052
exact
approximation (DEP)
approximation (REP)
-50
-30
-10
10
30
50
% Change in u for Actuator 1

Fig. 20

MAXIMUM VERTICAL DISPLACEMENT AT NODE 7

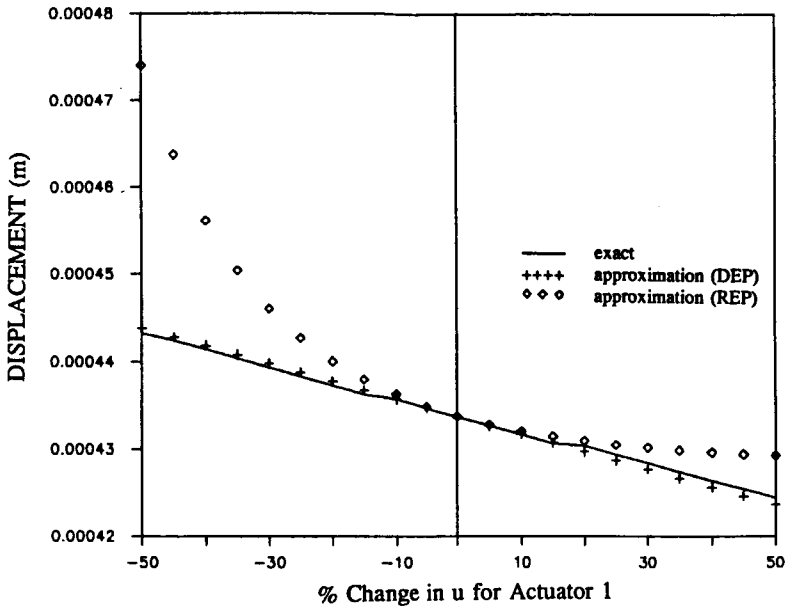

Fig. 21

MINIMUM VERTICAL DISPLACEMENT AT NODE 7

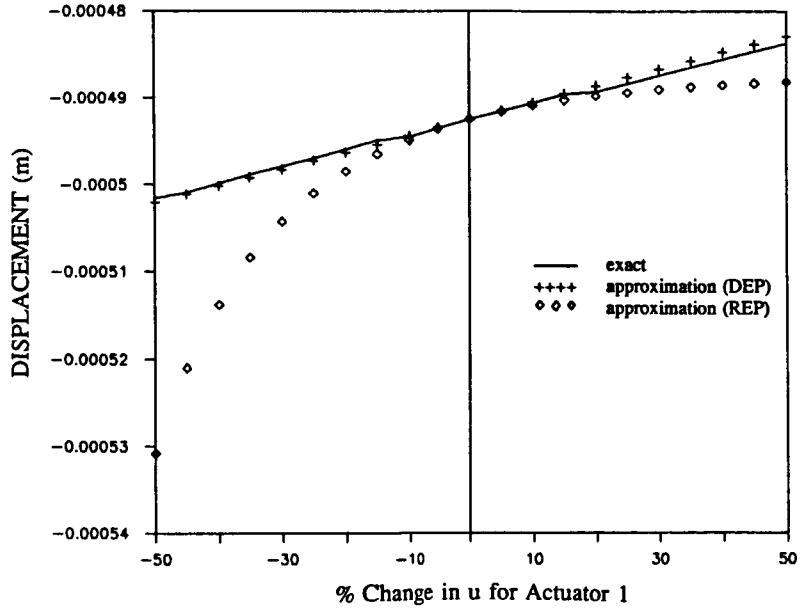

Fig. 22